IEEE Access
Multidisciplinary | Rapid Review | Open Access Journal

Received November 8, 2019, accepted November 21, 2019, date of publication November 25, 2019,
date of current version December 11, 2019.

Digital Object Identifier 10.1109/ACCESS.2019.2955803

Novel Bearing Current Suppression Approach in Doubly-Fed Induction Generators

RUIFANG LIU[1], ERLE YANG[1], JIAYAO CHEN[1], AND SHUANGXIA NIU[2]
[1]School of Electrical Engineering, Beijing Jiaotong University, Beijing 100044, China
[2]Department of Electrical Engineering, The Hong Kong Polytechnic University, Hong Kong

Corresponding author: Ruifang Liu (rfliu@bjtu.edu.cn)

This work was supported in part by the National Natural Science Foundation of China under Grant 51777008.

ABSTRACT Doubly-fed induction generators (DFIGs) are widely used in the wind power generation systems. However, due to the use of the power electronic devices, such as insulated gate bipolar transistor (IGBT), it is inevitable to generate a non-zero common mode voltage on the rotor side. The common mode voltage can induce the bearing voltage through the stray capacitances and result in the bearing currents, which seriously affect the efficiency and the safety of wind power generation system. This paper proposes a new bearing current suppression method in DFIGs. The key is to design the electrostatic shield on the rotor side of DFIGs and based on the bearing voltage ratio to effectively mitigate the bearing voltage ratio in the generator. This paper firstly investigates the bearing current equivalent circuit and the stray capacitance calculation method. The sensitivity analysis on the bearing voltage ratio is carried out, which shows that the capacitance between the rotor winding and the rotor core is a key parameter to mitigate the bearing voltage and bearing currents. The electrostatic shield on the rotor side of DFIGs is designed to regulate the capacitance value and hence the bearing currents. Finally, the bearing current of the converter-DFIG system is simulated and analyzed. The results verify that the new suppression method can effectively suppress the bearing currents.

INDEX TERMS Doubly-fed induction generators, bearing currents, bearing voltage ratio, mitigation approach.

I. INTRODUCTION

In recent years, with the increasing concern on energy crisis and air pollution, the development of renewable energy power generation technology has been strongly supported in lots of countries and areas. The clean energy power generation, especially solar power generation and wind power generation has increased rapidly. At present, many types of electric machine also can be used in the wind turbine application [1], [2], and the doubly-fed induction generator (DFIG) is one of the most widely used wind turbine forms in the wind turbine application. DFIGs adopt converter power supplies on rotor side, and the converter only needs 30% of the rated power and the whole cost of the system is greatly reduced. Due to the smaller converter capacity, smaller volume and lower cost, it has become a favored structure form for the wind power equipment manufacturers and operators [3], [4]. The schematic diagram of doubly-fed induction wind power generation system is shown in Figure 1.

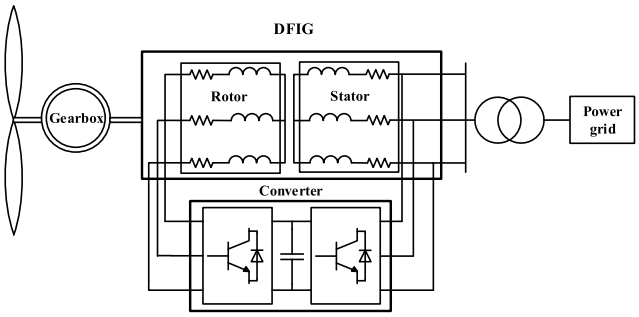

FIGURE 1. Doubly-fed induction wind power generation system.

However, due to the high-frequency switching device inside the converter in DFIGs system, there is also the high frequency common voltage produced to generate the bearing voltage through the internal stray capacitances. Then the bearing voltage generates the bearing currents following

The associate editor coordinating the review of this manuscript and approving it for publication was Xiaodong Sun.

through the bearings, which is also known as the bearing electric erosion. Especially, the discharge current may be generated when the bearing voltage between the inner raceway and the outer raceway exceeds the threshold voltage of the lubricant film, which would cause the occurrence of oil film breakdown. The heat of instantaneous discharge will induce the component of grease to deteriorate and cause pit erosion on the bearing surface, which would gradually induce the bearing premature failure. Consequently, it threatens the normal operation of the system, and contributes to unplanned and costly system downtime [5]. Compared with permanent magnet synchronous generators (PMSGs), and variable frequency induction motors, the bearing electric erosion in DFIG wind turbine system is much more serious due to the system construction of DFIGs. The converter of DFIG connects with the rotor winding, and the coupling between the rotor winding and the shaft is tighter, so the bearing voltage induced by the common mode voltage is more serious than the variable frequency induction motors and PMSGs [6], [7].

The bearing current problems have aroused widespread concern [7], [8]. Many control methods are investigated to suppress the bearing currents and address this bearing electric erosion problem. An improved PWM control strategy is proposed to suppress the common mode voltage and bearing voltage in [9]. Gerwin Preisinger, a bearing manufacturer, has proposed the bearing current suppression scheme for the mixed ceramic deep groove ball bearings [10]. In DFIGs, the brushes are widely used to eliminate the bearing voltage and the bearing currents. However, wind turbines are usually installed in places that are high above the ground, which causes the maintenance and overhaul of wind turbines complex and costly. Ceramic rolling elements bearings are expensive and the brushes need to maintain and periodic replacement. Therefore, it would be an economical and convenient method to suppress the bearing currents from the perspective of the motor manufacturing. In DFIGs system, the stray capacitances of the generator provide a low impedance path for common mode voltage transmission. Adding a shielding layer between the rotor winding and the rotor core can block the path. Based on this principle, a novel bearing currents mitigation method is proposed in this paper. The method can decrease the bearing early premature rate and the cost on maintenance, which will benefit the motor manufacturers and the wind power operators. The placement of the shielding layer of DFIG is different from which in variable frequency induction motors.

In this paper, the bearing current equivalent analysis model of DFIG is introduced firstly, and the method of calculating the stray capacitance parameters based on electromagnetic field is given. Then, the sensitivity analysis is carried out for the influence of capacitance parameters on bearing voltage, and the bearing current suppression of DFIGs based on rotor side electrostatic shielding is put forward. Finally, the effect of the novel method is verified by the simulation results.

II. BEARING CURRENT MODEL OF DFIG

A. THE COMMON MODE VOLTAGE GENERATED BY THE CONVERTER

The rotor winding of DFIGs connects to the converter, and the output voltage is a set of equal amplitude but different width high-frequency voltage pulses. The relationship between common mode voltage V_{com} and three-phase voltage V_u, V_v, and V_w is:

$$V_{com} = \frac{V_u + V_v + V_w}{3} \tag{1}$$

Different from the three-phase symmetric sinusoidal operation state, the sum of the three-phase voltage will not be zero at any moment in the converter pulse power supply mode, resulting in non-zero V_{com} between the rotor winding and the ground. The common mode voltage is a high-frequency pulse voltage, and its value is affected by the DC bus voltage and the frequency converter modulation method. The common mode voltage on the rotor side is applied between the rotor winding and the ground. The common mode voltage is the source of the bearing currents, and the internal stray capacitances of DFIG form the coupling channel of the common mode circuit.

B. THE BEARING CURRENT MODEL OF DFIG

In the DFIG, the stray capacitances have no influence at low frequency. However, they constitute the low impedance loop for the common mode voltage at high frequency [11]. There are four equivalent conductors in the DFIG, which are the stator winding, the rotor winding, the rotor core, and the stator core. The stator core connects to the frame and the rotor core connects to the shaft. Thus, the stator core and frame are at the same electric potential, and the rotor core and shaft are also at the same potential. When we ignore the effect of stator winding, there are three main stray capacitances in DFIGs, i.e. C_{rwf}, C_{rwr}, and C_{rf}. Among them, C_{rwf}, C_{rwr}, C_{rf} are the capacitance of the rotor winding to the frame, the capacitance of the rotor winding to the rotor core, and the capacitance of the rotor core to the frame respectively, whose specific distribution is shown in Figure 2.

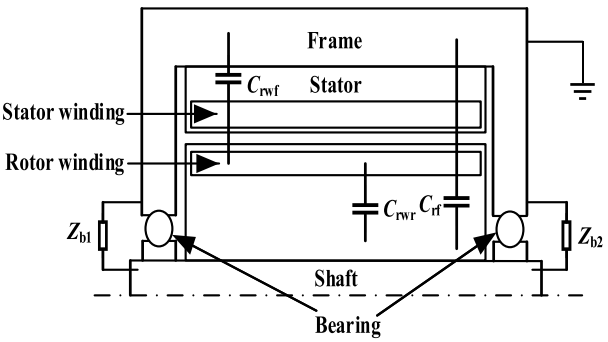

FIGURE 2. Stray capacitances distribution of DFIG.

In the condition that the stator frame properly grounds, the influence of the common mode voltage from the stator

side can be ignored [7]. The common mode circuit is shown in Figure 3.

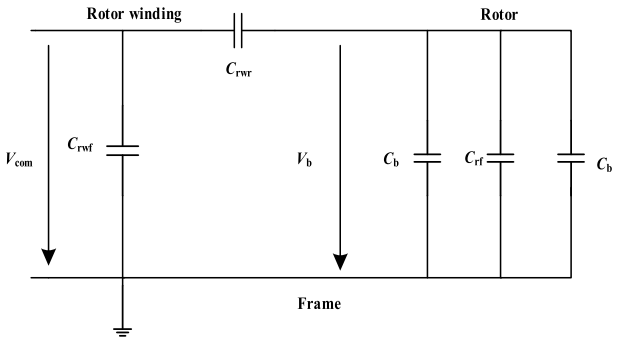

FIGURE 3. Common mode circuit of bearing current problem of DFIG.

In Figure 3, V_{com} is the common mode voltage of the converter. The bearing inner raceway connects the shaft, namely, the bearing inner raceway is at the same potential as the rotor core. The bearing outer raceway connects the stator end cover, namely, the outer raceway is at the same potential as the stator core and frame. Balls of the bearing separate the inner raceway and the outer raceway and the lubricating grease exists between the balls and raceways. The bearing can be taken as a capacitance when there is no discharge bearing currents. C_b is the equivalent bearing capacitance of the drive end or non-driven end.

The ratio of the bearing voltage V_b and the common mode voltage V_{com} can be defined as the bearing voltage ratio (BVR) [12], which is an indicator of bearing damage. According to the Figure 3, the BVR of the DFIG is shown in (2).

$$\lambda_{BVR} = \frac{V_b}{V_{com}} = \frac{C_{rwr}}{C_{rwr} + C_{rf} + 2C_b} \tag{2}$$

C. CALCULATION AND MEASUREMENT OF DFIG STRAY CAPACITANCES

We can see from the bearing current model of the DFIG that V_{com} is the excitation source of the bearing voltage, and the stray capacitances in the motor forms the coupling channel. The stray capacitances can be acquired by analytical calculation, finite element calculation, and measurement. The capacitor will be approximately treated as a plate capacitor or a cylindrical capacitor when we use analytical calculation [9], which cannot reveal the true generator structure. Moreover, in analytical calculation, each capacitance is treated as an independent one, so the electric field influence of different conductors cannot be considered. The theory of partial capacitance of multi-conductor system should be adopted to calculate the stray capacitances in generators. The finite element calculation of electromagnetic field can be used to solve the problem.

Taking a 1.5 MW DFIG as an example, and ignoring the end winding effect, we can build a 2D model with ANSYS Maxwell software based on the generator structure parameters, as shown in Figure 4. The parameter of the DFIG is shown in Table 1.

TABLE 1. The main parameters of the 1.5MW DFIG.

Parameters	Symbol	Value
Stator slot number	N_s	72
Rotor slot number	N_r	84
Length of iron core	L/mm	652
Air gap	δ/mm	2.5
Stator inner radius	R_s/mm	285
Rotor slot wedge thickness	d_{r2}/mm	4.5
Stator slot wedge thickness	d_{s2}/mm	4.5
Rotor slot insulation thickness	d_{rw1}/mm	1.35
Stator slot insulation thickness	d_{sw1}/mm	0.45
Rotor slot width	b_{r1}/mm	3
Stator slot width	b_{s1}/mm	15.2
Relative permittivity of slot wedge	ε_{r1}	3
Relative permittivity of slot insulation	ε_{r2}	3.4

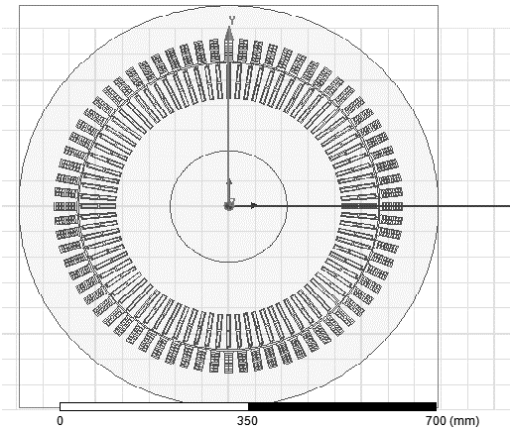

FIGURE 4. 2D model of a 1.5 MW DFIG.

The stator core is taken as the reference, and the rotor winding and rotor core are taken as the independent conductors applied different voltages. According to the theory of partial capacitance of multi-conductor system, we can get the relationship between the capacitances and the potential [13], as shown in (3).

$$\begin{bmatrix} q_{rw} \\ q_r \end{bmatrix} = [\beta] \begin{bmatrix} \varphi_{rw} \\ \varphi_r \end{bmatrix} \tag{3}$$

where the subscript rw indicates the rotor winding, r indicates the rotor core, q_{rw}, q_r are the charges of the rotor winding and rotor core respectively, φ_{rw}, φ_{rw} are the potential of the rotor winding and the rotor core respectively, and $[\beta]$ is the electrostatic induction coefficient matrix, which contains following elements:

$$[\beta] = \begin{bmatrix} C_{rwf} + C_{rwr} & -C_{rwr} \\ -C_{rwr} & C_{rf} + C_{rwr} \end{bmatrix} \tag{4}$$

When adopting the electrostatic field solver in ANSYS Maxwell, we can get the electrostatic induction coefficient matrix. Then we can get the values of the capacitance C_{rwf}, C_{rwr}, C_{rf}. To acquire the actual results, the values of

capacitance should multiply the effective axial length of the generator.

The stray capacitances of the motor are also measured. The instrument is an Agilent U1733C handhold LCR tester. Using two probes of capacitance meter to touch any two equivalent electrodes, we can measure the equivalent capacitance between any two ports, and then we can acquire the stray capacitances. Table 2 shows the finite element numerical calculation results and the measured results of the stray capacitances of the DFIG.

TABLE 2. Calculated and measured capacitances of a 1.5mw DFIG.

Parameters	C_{rwf}	C_{rwr}	C_{rf}
Calculated value /nF	0.027	152.3	3.3
Measured value /nF	0.43	153.0	3.96

It is shown from Table 2 that C_{rwr} is the largest capacitance. This is because C_{rwr} is the capacitance between the rotor winding and the rotor core, the insulation distance is small, and the dielectric constant is large. Capacitances C_{rf}, C_{rwf} are relatively small, because these capacitances are between the stator and rotor side conductors, the distance between the equivalent electrodes is large, and the equivalent electrode area is small.

The calculation results are compared with the measured results, and the errors of C_{rf}, C_{rwf} showed that the calculation values are less than the measured values. The reason for the error may be that the calculation model adopts the 2D model, which neglects the influence of the winding end. To obtain the accurate results, the 3D model needs to be used. However, the 2D calculation model is simple, and the calculation efficiency is high, and the calculation results have a certain reference value. The measured values of capacitance parameters are used in the simulation analysis of bearing currents.

D. SENSITIVITY ANALYSIS OF BERAING VOLTAGE RATIO

The bearing voltage ratio is an important index for measuring the damage of motor bearings. Taking the bearing capacitance C_b as 0.12 nF, the bearing voltage ratio can be calculated as 96.6% according to (2). If the common mode voltage is close to the DC Bus voltage, the bearing voltage will cause serious harm to the bearing.

The relationship between the stray capacitances and the bearing voltage ratio can provide the guidance for the suppression measures of bearing currents.

For the industrial variable frequency motor, the BVR is less than 10%. It is because the inverter is applied to the stator windings of the induction motors. Due to the distance of the airgap, the capacitance between the stator winding to the rotor is very small, which determines the BVR in variable frequency induction motor is also small. However, in DFIG, the converter connects to the rotor winding, and the capacitance C_{rwr} is larger than correspondent capacitance in the induction motors. It leads to the BVR in the DFIG is much larger than that of the variable frequency induction motor.

The relationship between the stray capacitances of DFIG and the bearing voltage ratio can provide the guidance for the suppression measures of bearing currents. Taking the 1.5MW DFIG as an example, we analyzed the sensitivity of each parameter to the bearing voltage. We could see from (2) that C_{rwr}, C_b, C_{rf} have an influence on the bearing voltage. C_{rf} is the stator core to rotor core capacitance, and the main design size of the DFIG is not easy to change, and the influence of C_{rwr} and C_{rf} on the BVR is shown in Figure 5.

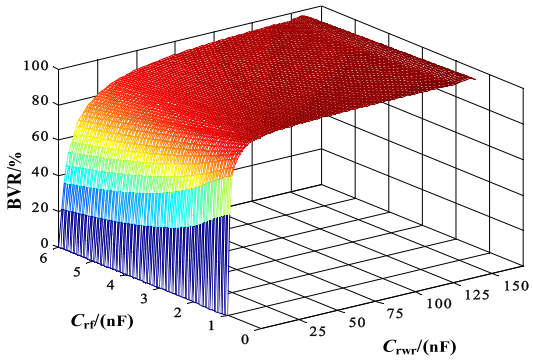

FIGURE 5. The influence of C_{rwr} and C_{rf} on bearing voltage ratio.

It is shown that C_{rwr} has an obvious influence on the BVR. With the decreasing of C_{rwr}, the bearing voltage decreases significantly. If the capacitance C_{rwr} can be reduced, the bearing voltage and bearing currents could be suppressed.

III. THE SUPPRESSION METHOD OF BEARING CURRENT OF DFIG BASED ON ELECTROSTATIC SHIELDING

At present, the suppression methods of the bearing currents of the DFIG mainly adopt the shaft connecting brush and insulated bearings. For the grounding brush, it requires regular maintenance and replacement. While the wind turbines are located at high altitude, the cost of maintenance and replacement of the brush is relatively high. For the isolated bearings, their cost is high and effect is limited. If the DFIG can suppress the bearing currents more effectively from the design, a new breakthrough will be made. In this paper, the electrostatic shielding suppression method at rotor-side was put forward. According to Figure 5, the variation of the capacitance C_{rwr} is sensitive to the BVR. Reducing the coupling between the rotor core and the rotor winding can reduce the value of the BVR, thereby reducing the probability of bearing breakdown discharge. If the shielding layer is inserted between the rotor core and the rotor winding, the isolation of the two conductors can be realized, and C_{rwr} can be reduced and even be zero. If C_{rwr} is 0, the coupling pathway can be separated, and the bearing currents can be eliminated.

Previously adding the shielding was discussed to suppress bearing currents of the variable frequency induction motors [14]. To suppress the circulating bearing currents, the shielding layer was placed between the stator winding and

stator core [15]. To suppress the electric discharge machining (EDM) bearing currents, the shielding layer should be put between the stator winding and the rotor winding [16]. However, in DFIGs the rotor winding connects to the convertor. The coupling between the rotor winding and rotor core is generated by the capacitance C_{rwr}. In order to isolate the two parts, the shielding layer should be placed between the rotor winding and the rotor core. The shielding scheme is shown in Figure 6.

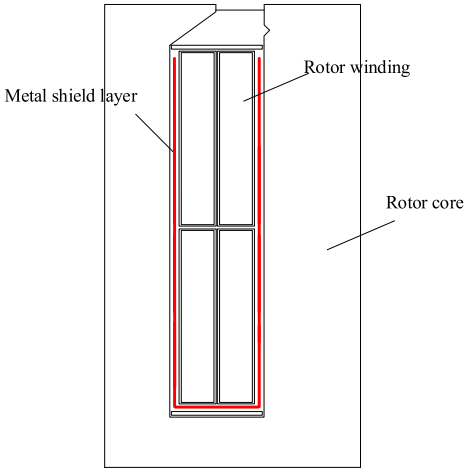

FIGURE 6. The position of the metal shielding layer in rotor slots.

A. THE INFLUENCE OF THE CHANGE OF SHIELDING LAYER STRUCTURE ON SUPPRESSION EFFECT

To ensure the efficiency of the motor and reduce the cost of production, it is necessary to use its geometry space on the basis of ensuring the efficiency of the motor, and discuss the thickness of the shielding layer on the suppression effect. The shielding layer thickness was set as 0.16, 0.32, 0.48mm respectively, and the finite element calculation was carried out. The stray capacitances and BVR under different shielding layers can be obtained through (2). The results are listed in Table 3.

TABLE 3. Finite element calculation results on stray capacitances with different shielding layer thickness.

Parameters/ nf	without shielding layer	the thickness of shielding layer		
		0.16mm	0.32mm	0.48mm
C_{rwf}	0.027	258.7	314.86	412.25
C_{rwr}	152.3	6.4	6.06	5.7
C_{rf}	3.3	1097.76	1495.02	1505.43
BVR	94.8%	0.430%	0.404%	0.377%

With the shielding layer, the coupling capacitance C_{rwr} between the rotor winding and the rotor core will be reduced significantly. Meantime, the distance between rotor winding and the stator frame (the ground) decreases, and the effective area increases, which causes coupling capacitance C_{rwf} increase, but it will not affect the BVR. We can see that there is no obvious change with 3 different thickness shielding layers, and the values of BVR are also very closely. But the BVR is far less than 94.8% when there is no shielding layer. The change of shielding layer thickness has little effect on the shielding effect, so the thickness of shielding layer can be minimized to reduce the space usage and the cost.

B. THE INFLUENCE OF SHIELDING LAYER SEGMENTATION ON SUPPRESSION EFFECT

According to the shielding theory, when the shielding layer adopts the grating structure, it can still have a shielding effect. If the shielding layer is not a complete conductor, there will be little amount electric coupling existed between the two isolated conductors. The coupling capacitance with the incomplete shielding layer will be larger than the complete one. But shield segmentation can reduce eddy current losses in shielding layer. In this case, the influence of segmentation on the shielding effect was discussed. A shielding layer with a thickness of 0.32mm was divided into 3 segments, 9 segments and 13 segments respectively, which were distributed evenly in the rotor slot. For example, the shielding layer is divided into 9 segments, as shown in Figure 7.

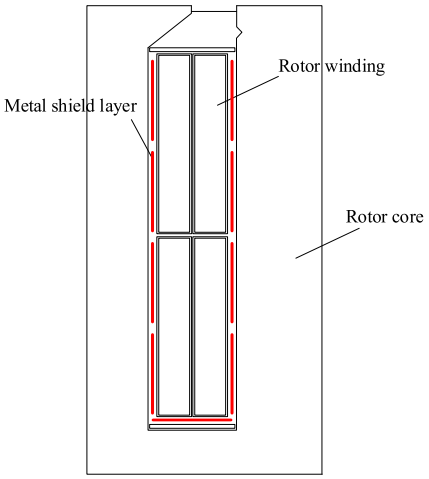

FIGURE 7. The model of shielding layer with 9 segments.

The finite element calculations on different segments were performed. The stray capacitances of DFIG with different shielding layer segments were calculated, the values of capacitance and BVR were shown in Table 4. The results show that the BVR of the unsegmented shield condition is lowest one. With the increase of the segment number, the capacitance C_{rwr} increases and the BVR gets bigger, accordingly.

C. ANALYSIS OF EDDY CURRENT LOSS UNDER THE CONDITION WITH THE SHIELDING LAYER

When the metal shielding layer is inserted to the rotor slots, the eddy current loss on the metal shielding layer would be caused by alternating magnetic field. The eddy current loss can be analyzed and calculated with finite element analysis.

When the rotor rotates, the rotating magnetic field in the motor always rotates with the synchronous speed, and

TABLE 4. Finite element calculation results on stray capacitances with different shielding layer segments.

Parameters/ nf	unsegmented	3 segments	9 segments	13 segments
C_{rwf}	314.86	312	275.6	255.4
C_{rwr}	6.06	6.4	29	39.3
C_{rf}	1495.2	1492.1	1251.7	1155.86
BVR	0.404%	0.447%	2.3%	3.3%

the inner shielding layer of the rotor rotates with the rotor. Therefore, the relative rotation speed between the shield layer and the rotating magnetic field is the slip speed. The eddy current frequency of the shielding layer is the slip frequency. If the three-phase symmetrical current of the slip frequency is applied in the winding, the eddy current loss during rated operation can be obtained after the magnetic density distribution at the rated operation is reached.

We take a 1.5 MW DFIG as an example. The slip frequency is set to 8.5 Hz. The eddy current loss of the unsegmented metal shield layer was calculated and the result is 1323.4 W, which accounts for about 0.088% of the total power. The magnetic field distribution is shown in Figure 8. And the eddy current losses of different segmented shield layers are calculated through the same way, the values of which are as shown in Table 5.

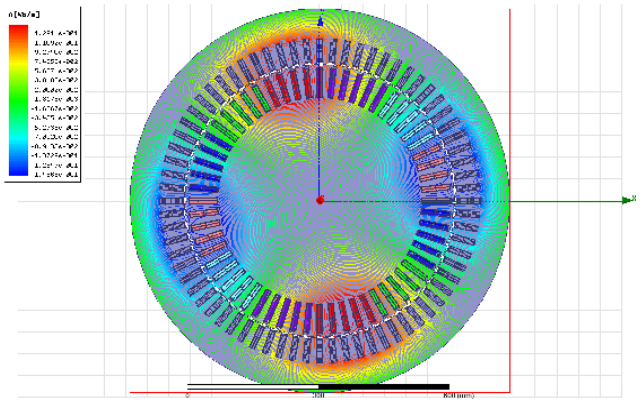

FIGURE 8. The magnetic field distribution of the DFIG with shielding layer.

TABLE 5. Eddy current lossES of different shielding layer segments.

Number of segments	unsegmented	3 segments	9 segments	13 segments
Eddy loss/W	1323.4	1304.6	1218.0	898.6

When the DFIG works at the rated speed, the slip frequency of the rotor winding is relatively low, and the eddy current loss on the metal shielding layer is smaller. As the number of segments of the shield increases, the eddy current loss decreases.

It is shown from the calculation that the BVR can be decreased obviously, and it will have a good effect on the bearing current suppression. However, in the engineering practice, it is necessary to combine the specific manufacturing process, such as the thickness of the shielding layer and the realization of grounding the metal shielding layer, which need to be further studied.

IV. PREDICTION OF THE BEARING CURRENT OF DFIG

After obtaining the stray capacitances of the DFIG, the bearing voltage and bearing currents can be predicted by using the bearing current equivalent circuit. The bearing current simulation circuit model of the DFIG was established through MATLAB/ Simulink R2014a, (Mathworks, Natic, MA, USA.), as shown in Figure 9. Then the bearing voltage and bearing currents can be predicted. The rotor winding three-phase resistance and inductance are represented by R and L respectively. To simplify the problem, only the capacitance breakdown of one side of the bearing was analyzed. The equivalent switch k_1 and k_2 is used to simulate the breakdown of the bearing oil film when the bearing voltage is over the threshold voltage. The switch k_1 closes and k_2 is disconnected when the oil film is not broken down, and the bearing acts as a capacitance. When the oil film is broken down, the switch k1 is off and k2 is closed, and the bearing is presented as an equivalent breakdown resistance.

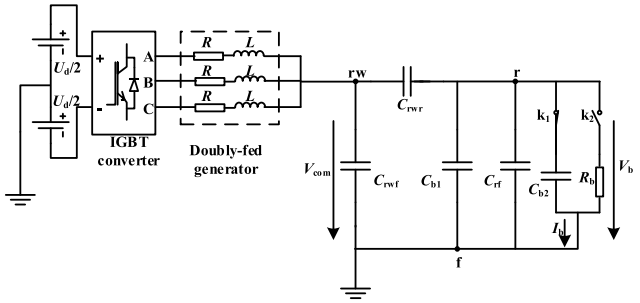

FIGURE 9. The simulation circuit of bearing currents of DFIG.

The Carrier frequency f is 5 kHz, the measured stray capacitances of DFIG are as shown in Table 2, the bearing capacitances C_{b1} and C_{b2} are both 120 pF, the bearing equivalent breakdown resistance R_b is 10Ω, and the breakdown threshold voltage of bearing is set to 15 V. The logic module is used to simulate the breakdown of bearing oil film. The common mode voltage V_{com}, bearing voltage V_b and bearing current I_b were acquired from the simulation, as shown in Figure 10.

In Figure 10, the BVR is not same as the calculated value because of the discharge breakdown of the bearing oil film. The peak value of V_{com} is about 600V, and the peak value of V_b is about 200V. The bearing discharge current reaches 18A, and such a large bearing current will seriously affect the bearing lifetime.

The bearing currents under adopting the shielding layer are also simulated. The thickness of the shielding layer is set to 0.32 mm. The structures of the shielding layer are set to the unsegmented shielding, 3 segments shielding,

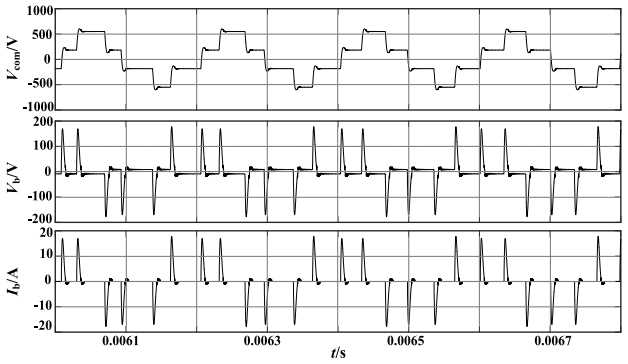

FIGURE 10. Simulation results of common mode voltage V_{com}, bearing voltage V_b and bearing current I_b without the shielding layer.

9 segments shielding, 13 segments shielding respectively. Here, the simulation diagrams of continuous shielding are shown in Figure 11. And the simulation results are shown in Table 6.

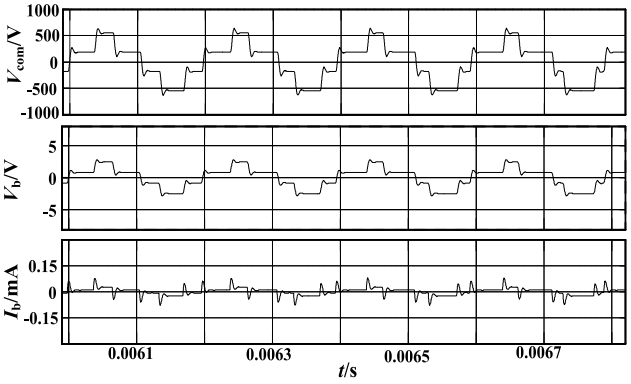

FIGURE 11. Common mode voltage V_{com}, bearing voltage V_b and bearing current I_b with the shielding layer.

TABLE 6. The peak of bearing voltage and bearing current of different shielding layer segments.

Number of segments	unsegmented	3 segments	9 segments	13 segments
Bearing voltage/V	2.5	2.7	14	20.7
Bearing current/mA	0.10	0.12	0.60	200

When the continuous shielding is adopted, the peak of bearing voltage is 2.5V, and the bearing current is reduced to approximately 0.1mA, which can be seen that the bearing current of the double-fed induction wind turbines is effectively suppressed when the rotor electrostatic shielding method is adopted. As the number of segments in the shield increases, the shielding effect is gradually weakened, but there is still a suppression effect.

Then, we simulate the bearing current with the shielding layer using different thickness, 0.16 mm, 0.32 mm, 0.48mm, and the structures are continuous shielding. The simulation results of the peak of the bearing voltage and the bearing current are shown in Table 7.

TABLE 7. The peak of bearing voltage and bearing current of different shielding layer thickness.

Thickness of the shielding layer/mm	0.16	0.32	0.48
Bearing voltage/V	3.7	2.5	2.3
Bearing current/mA	0.14	0.10	0.07

As shown in Table 7, as the thickness of shielding layer has less influence on the bearing voltage and the bearing current. Therefore, in order to reduce space use and cost, the thickness of shielding layer can be minimized.

According to the above analysis, the thin complete shielding layer could effectively suppress the bearing currents. The extra cost of the new method cost is related to both the material usage of the shielding layer and the manufacturing technology. The latter one needs to be analyzed during the manufacture process. We will do thorough work on it in the future research.

V. CONCLUSION

DFIG is one of the mainstream types of the wind turbines, but the bearing current problem due to the variable frequency power supply causes serious damage to its safe operation. In this paper, a novel bearing current mitigation approach based on the electrostatic shield design on rotor side was proposed after the sensitivity analysis on the BVR. It's the first time the shielding method is introduced to suppress the bearing currents in DFIGs. The thickness and the segmentation of shielding layer and the eddy current loss on the shielding layer are also discussed. The results showed that the new suppression method can effectively suppress the bearing currents. The suppression effect is better under unsegmented condition, but the eddy current loss is bigger under this condition. An optimization scheme considering the suppressing effect, eddy current loss and the manufacturing cost under the allowable bearing currents will be considered in the future. The detail experimental verification will be carried out in our future research.

REFERENCES

[1] X. Sun, K. Diao, G. Lei, Y. Guo, and J. Zhu, "Study on segmented-rotor switched reluctance motors with different rotor pole numbers for BSG system of hybrid electric vehicles," *IEEE Trans. Veh. Technol.*, vol. 68, no. 6, pp. 5537–5547, Jun. 2019, doi: 10.1109/TVT.2019.2913279.

[2] Z. Shi, X. Sun, Y. Cai, Z. Yang, G. Lei, Y. Guo, and J. Zhu, "Torque analysis and dynamic performance improvement of a PMSM for EVs by skew angle optimization," *IEEE Trans. Appl. Supercond.*, vol. 29, no. 2, pp. 1–5, Mar. 2019.

[3] Y. He, J. Hu, and X. Lie, "Overview of modern wind power technology," in *Grid-Connected Doubly-Fed Asynchronous Wind Turbine Operation Control*, 1st ed. Beijing, China: China Electric Power Press, 2012, pp. 7–11.

[4] J. Zitzelsberger, W. Hofmann, A. Wiese, and P. Stupin, "Bearing currents in doubly-fed induction generators," in *Proc. Eur. Conf. Power Electron. Appl.*, Dresden, Germany, Sep. 2005, pp. 11–14.

[5] Z. Li, X. Ma, K. Dong, W. Shen, and W. Zhao, "Study and discussion on the problems of shaft voltage and bearing current in wind power generation system," in *Proc. 9th IEEE Conf. Ind. Electron. Appl.*, Hangzhou, China, Jun. 2014, pp. 1696–1700.
[6] M. Whittle, J. Trevelyan, and P. J. Tavner, "Bearing currents in wind turbine generators," *J RENEW SUSTAIN ENER*, vol. 5, no. 5, 2013, Art. no. 053128, doi: 10.1063/1.4822048.
[7] J. Adabi, F. Zare, A. Ghosh, and R. D. Lorenz, "Calculations of capacitive couplings in induction generators to analyse shaft voltage," *IET Power Electron.*, vol. 3, no. 3, pp. 379–390, May 2010.
[8] S. Xing and Z. Wu, "Characteristic research of bearing currents in inverter-motor drive systems," in *Proc. CES/IEEE 5th Int. Power Electron. Motion Control Conf.*, Shanghai, China, Aug. 2006, pp. 1–4.
[9] M. E. Adabi and A. Vahedi, "A survey of shaft voltage reduction strategies for induction generators in wind energy applications," *Renew. Energy*, vol. 50, pp. 177–187, Feb. 2013.
[10] P. Gerwin, "SKF large hybrid ceramic deep groove ball bearings—A reliable solution for wind turbines," (in Chinese), *Motor Control Appl.*, vol. 35, no. 12, pp. 54–57, Dec. 2018.
[11] R. F. Liu, X. Ma, X. Ren, J. Cao, and S. Niu, "Comparative analysis of bearing current in wind turbine generators," *Energies*, vol. 11, no. 5, p. 1305, May 2018.
[12] A. Muetze, J. Tamminen, and J. Ahola, "Influence of motor operating parameters on discharge bearing current activity," *IEEE Trans. Ind. Appl.*, vol. 47, no. 4, pp. 1767–1777, Jul./Aug. 2011.
[13] G. Z. Ni, "Static electromagnetic field I: Electrostatic field," in *Principle Of Engineering Electromagnetic Field*, Beijing, China: Higher Education Press, 2002, pp. 94–96.
[14] D. Busse, J. Erdman, R. J. Kerkman, D. W. Schlegel, and G. L. Skibinski, "An evaluation of the electrostatic shielded induction motor: A solution for rotor shaft voltage buildup and bearing current," in *Proc. IEEE Ind. Appl. Conf. 31st IAS Annu. Meeting*, Oct. 1996, pp. 610–617.
[15] K. Vostrov, J. Pyrhönen, J. Ahola, and M. Niemelä, "Non-circulating bearing currents mitigation approach based on machine stator design options," in *Proc. 13th Int. Conf. Elect. Mach. (ICEM)*, Alexandroupoli, Greece, Sep. 2018, pp. 866–872.
[16] P. Maki-Ontto and J. Luomi, "Bearing current prevention of converter-fed AC machines with a conductive shielding in stator slots," in *Proc. IEEE Int. Electr. Mach. Drives Conf.*, Madison, WI, USA, Jun. 2003, pp. 274–278.

RUIFANG LIU received the B.S. and M.S. degrees in electrical engineering from the Taiyuan University of Technology, Taiyuan, China, and the Ph.D. degree from the Department of Electrical Engineering, Southeast University, China. Since 2003, she has been with Beijing Jiaotong University, China, where she is currently an Associate Professor with the School of Electrical Engineering. Her research interests include the integration analysis of power electronic and electrical machine systems, electrical machine performance analysis, electromagnetic field theory, and numerical calculation.

ERLE YANG received the B.S. degree in electrical engineering from Tibet University, China, in 2018. He is currently pursuing the M.S. degree with the School of Electrical Engineering, Beijing Jiaotong University. He is involved in the integration analysis of power electronics and motor systems, electromagnetic field theory, and numerical calculation.

JIAYAO CHEN received the B.S. and M.S. degrees in electrical engineering from Beijing Jiaotong University, in 2012 and 2016, respectively. He was involved in the integration analysis of power electronics and motor systems, electromagnetic field theory, and numerical calculation.

SHUANGXIA NIU received the B.Sc. and M.Sc. degrees in electrical engineering from the School of Electrical Engineering and Automation, Tianjin University, Tianjin, China, and the Ph.D. degree in electrical engineering from the Department of Electrical and Electronic Engineering, The University of Hong Kong, Hong Kong. Since 2009, she has been with The Hong Kong Polytechnic University, Hong Kong, where she is currently an Associate Professor with the Department of Electrical Engineering. She has authored or coauthored over 100 articles in leading journals. Her research interests include novel electrical machines and drives, renewable energy conversion systems, and applied electromagnetics.